Supplementary Online Content

Heck A, Fastenrath M, Coynel D, et al. Genetic analysis of association between calcium signaling and hippocampal activation, memory performance in the young and old, and risk for sporadic Alzheimer disease. *JAMA Psychiatry*. Published online September 2, 2015. doi:10.1001/jamapsychiatry.2015.1309.

This supplementary material has been provided by the authors to give readers additional information about their work.

eAppendix.

Detailed description of testing procedure in the Discovery sample:

Subjects were presented 24 neutral, 24 positive and 24 aversive photographs in a random order. The photographs were taken from the international affective picture system (IAPS)[1] and from an in-house database for eight of the neutral pictures that allowed us to equate the pictures for visual complexity and content (e.g., human presence). Pictures received from IAPS were classified according to the IAPS valence rating; the remaining eight pictures were rated based on an in-house valence rating. On the basis of normative valence scores (from 1 to 9), pictures were assigned to negative (2.3 ± 0.6), neutral (5.0 ± 0.3), and positive (7.6 ± 0.4) conditions, resulting in 24 pictures for each valence. Four additional pictures showing neutral objects were used to control for primacy and recency effects in memory. Two of these pictures were presented in the beginning and two at the end of the picture task. Pictures were presented for 2.5 s each. In addition, 24 scrambled pictures were used. The background of the scrambled pictures contained the color information of all pictures used in the experiment (except primacy and recency pictures), overlaid with a crystal and distortion filter (Adobe Photoshop CS3). In the foreground, a mostly transparent geometrical object (rectangle or ellipse of different sizes and orientations) was shown.

Immediately following the presentation of each photograph, subjects were asked to rate it for valence (negative, neutral, positive) and arousal (large, medium, small) on a three-point rating scale (Self Assessment Manikin, SAM). Free recall, reflecting EM performance, was tested 10 min after presentation of all photographs. To document performance for the delayed recall of positive, negative, and neutral pictures, subjects had to describe in writing each picture

with a few words. A picture was judged as correctly recalled if the rater could identify the presented picture based on the subject's description. Two blinded investigators independently rated the descriptions for recall success (inter-rater reliability > 99%). For the pictures, which were judged differently by the two raters (i.e. a particular picture was judged as correctly recalled by one rater but not the other), a third independent and blinded rater made a final decision with regard to whether the particular picture could be considered as successfully recalled.

Detailed description of testing procedure in the Replication sample:

The delayed free recall was performed outside of the scanner, 10 min after presentation of all photographs. Stimuli consisted of the same 72 pictures and 24 scrambled pictures as in the discovery sample.

The pictures were presented for 2.5 s in a quasi-randomized order so that at maximum four pictures of the same category occurred consecutively. A fixation cross appeared on the screen for 500 ms before each picture presentation. Trials were separated by a variable intertrial period of 9–12 s (jitter) that was equally distributed for each stimulus category. During the intertrial period, participants subjectively rated the picture showing scenes according to valence (negative, neutral, positive) and arousal (large, medium, small) on a three-point scale (SAM). For scrambled pictures, participants rated form (vertical, symmetric or horizontal) and size (large, medium, small) of the geometrical object in the foreground.

Detailed description of testing procedure in the Zurich sample:

Subjects were presented with 10 neutral, 10 positive and 10 aversive photographs in a quasi-randomized order. The photographs were taken from the international affective picture system

(IAPS) [1] and were presented for 4 s each. Immediately following the presentation of each photograph, subjects were asked to rate it for valence and arousal using the IAPS rating scales. Free recall, reflecting EM performance, was tested 10 min after presentation of all photographs. To document performance for the delayed recall of positive, negative, and neutral pictures, subjects had to describe in writing each picture with a few words. A picture was judged as correctly recalled if the rater could identify the presented picture based on the subject's description. Two blinded investigators independently rated the descriptions for recall success (inter-rater reliability > 99%). For the pictures, which were judged differently by the two raters (i.e. a particular picture was judged as correctly recalled by one rater but not the other), a third independent and blinded rater made a final decision with regard to whether the particular picture could be considered as successfully recalled.

Detailed description of the AgeCoDe sample

Briefly, participants were recruited between January 2003 and November 2004 in six German study centers (Bonn, Düsseldorf, Hamburg, Leipzig, Mannheim, Munich) via general practitioners (GP) connected to the respective study sites. Inclusion criteria were age of 75 years and older, absence of dementia (according to the GP’s judgment) and at least one contact with the GP within the last 12 months. Exclusion criteria were GP consultations by home visits only, residence in a nursing home, presence of a severe illness with an anticipated fatal outcome within three months, insufficient German language abilities, deafness or blindness, lack of ability to provide an informed consent and status as being only an occasional patient of the participating GP. A total of 3327 subjects were successfully

contacted and assessed with structured clinical interviews at their homes. A total of 110 individuals were excluded after the first interview due to presence of dementia or an actual age below 75 (falsely classified as 75 or older in the sample selection process). For the present analyses, data from baseline and three follow-up measurements with 18 months intervals were available. In a primary care-based sample of older individuals, conditions can be present that affect cognition and the reliability of neuropsychological tests. In order to generate a sample of healthy elderly individuals we further employed the following selection criteria at baseline: Age between 75 and 90 years, German as native language, at least school-leaving certificate, absence of severe hearing or vision impairments, absence of insufficient test motivation as judged by the interviewer, absence of disturbing factors during neuropsychological testing and absence of all of the following comorbid conditions: Parkinson's disease, epilepsy, alcohol abuse, stroke, multiple sclerosis, evidence of depression (a score of 6 or higher on the Geriatric Depression Scale), traumatic brain injury with unconsciousness of more than 30 min., visible neurological malfunctions and dementia according to DSM-IV criteria. In addition, we excluded subjects who converted to dementia up to the third follow-up or without neuropsychological test data available on baseline and all follow-up visits. After application of these selection criteria, a total of 1244 subjects remained in the sample. Sufficient DNA-samples for genome-wide genotyping were available for 782. Further 19 subjects were excluded due to sex-check inconsistencies. The final sample comprises 763 subjects (67.8% female; mean age: 79.5 ± 3.02). Delayed recall performance as quantified by the Consortium to Establish a Registry for Alzheimer’s Disease (CERAD) battery[2] served as phenotype. Subjects were presented a list of 10 words three times (presentation per word: 2 s), each time presented in a different order. After each run, subjects

freely recalled as many words as possible. The number of correctly remembered items (free recall) after a 10 min delay served as the phenotypic measure.

AD sample

International Genomics of Alzheimer's Project (IGAP) is a large two-stage study based upon genome-wide association studies (GWAS) on individuals of European ancestry.[3] In stage 1, IGAP used genotyped and imputed data on 7055881 single nucleotide polymorphisms (SNPs) to meta-analyze four previously-published GWAS datasets consisting of 17008 Alzheimer's disease cases and 37154 controls (The European Alzheimer's disease Initiative – EADI the Alzheimer Disease Genetics Consortium – ADGC The Cohorts for Heart and Aging Research in Genomic Epidemiology consortium – CHARGE The Genetic and Environmental Risk in AD consortium – GERAD). In stage 2, 11632 SNPs were genotyped and tested for association in an independent set of 8572 Alzheimer's disease cases and 11312 controls. Finally, a meta-analysis was performed combining results from stages 1 & 2.

Array-based SNP genotyping:

Briefly, genomic DNA concentration was determined by using a Nano-Drop ND-1000 and adjusted to 50ng/µl in water. 250ng of DNA was digested in parallel with 10 units of Sty I and Nsp I restriction enzymes (New England Biolabs, Beverly, MA) for 2 h at 37°C. Enzyme specific adaptor oligonucleotides were then ligated onto the digested ends with T4 DNA Ligase for 3 h at 16°C. After adjustment to 100µl with water, 10µl of the diluted ligation reactions were subjected to PCR. Three PCR reactions of 100µl were performed for Sty digested products and four PCR reactions for Nsp. PCR was performed with Titanium Taq

DNA Polymerase (Clontech, Mountain View, CA) in the presence of 4.5 μM PCR primer 002 (Affymetrix), 350 μM each dNTP (Clontech), 1M G-C Melt (Clontech), and 1X Titanium Taq PCR Buffer (Clontech). Cycling parameters were as follows: initial denaturation at 94°C for 3 min, amplification at 94°C for 30 s, 60°C for 45 s and extension at 68°C for 15 s repeated a total of 30 times, final extension at 68°C for 7 min. Reactions were then verified to migrate at an average size between 200-1100 bps using 2% TBE gel electrophoresis. PCR products were combined and purified with the Filter Bottom Plate (Seahorse Bioscience, North Billerica, MA) using Agencourt Magnetic Beads (Beckman Coulter, Fullerton, CA). Purified PCR products were quantified on a Zenith 200rt microplate reader (Anthos-Labtec, Cambridge, UK). 4 to 5μg/μl were obtained on average for each sample. From this stage on, the SNP Nsp/Sty 5.0/6.0 Assay Kit (Affymetrix) was used. Around 250 μg of purified PCR products were fragmented using 0.5 units of DNAse I at 37°C for 35 min. Fragmentation of the products to an average size less than 180 bps was verified using 4% TBE gel electrophoresis. Following fragmentation, the DNA was end labeled with 105 units of terminal deoxynucleotidyl transferase at 37°C for 4 h. The labeled DNA was then hybridized onto Genome-Wide Human SNP 6.0 Array at 50°C for 18 h at 60 rpm. The hybridized array was washed, stained, and scanned according to the manufacturer's (Affymetrix) instructions using Affymetrix GeneChip Command Console (AGCC, version 3.0.1.1214). Generation of SNP calls and Array quality control were performed using the command line programs of the Affymetrix Power Tools package (version: apt-1.14.4.1). According to the manufacturer's recommendation, contrast QC was chosen as QC metric, using the default value of greater or equal than 0.4. All samples passing QC criteria were subsequently genotyped using the Birdseed (v2) algorithm. Mean Call Rate for all samples averaged >98.5%. This value refers

to per sample (i.e. individual) call rate, and ranged from 95.1% to 99.7%. Thus, no individual with a SNP call rate below 95% was included.

MRI acquisition: Measurements were performed on a Siemens Magnetom Verio 3 T whole-body MR unit equipped with a twelve-channel head coil. Functional time series were acquired with a single-shot echo-planar sequence using parallel imaging (GRAPPA). We used the following acquisition parameters: TE (echo time)=35 ms, FOV (field of view)=22 cm, acquisition matrix=80 × 80, interpolated to 128 × 128, voxel size: 2.75 × 2.75 × 4 mm^3, GRAPPA acceleration factor R=2.0. Using a midsagittal scout image, 32 contiguous axial slices placed along the anterior–posterior commissure (AC–PC) plane covering the entire brain with a TR=3000 ms (α=82°) were acquired using an ascending interleaved sequence. The first two acquisitions were discarded due to T1 saturation effects. A high-resolution T1-weighted anatomical image was acquired using a magnetization prepared gradient echo sequence (MPRAGE, TR=2000 ms; TE=3.37 ms; TI=1000 ms; flip angle=8; 176 slices; FOV= 256 mm; voxel size=1 x 1 x 1 mm^3).

Detailed description of fMRI preprocessing and first level analyses:

Normalization incorporated the following steps. (1) Structural images of each subject were segmented using the ‘‘New Segment’’ procedure in SPM8. (2) The resulting gray and white matter images were used to derive a study-specific group template. The template was computed based on a subset of 1000 subjects of the replication sample. (3) An affine transformation was applied to map the group template to MNI space. (4) Subject-to-template and template-to-MNI transformations were combined to map the functional images to MNI space. The functional images were smoothed with an isotropic 8 mm full-width at half-

maximum (FWHM) Gaussian filter. Intrinsic autocorrelations were accounted for by AR(1) and low-frequency drifts were removed via high-pass filter (time constant 128 s). Regressors modeling the onsets and duration of stimulus events were convolved with a canonical hemodynamic response function. More precisely, the model comprised regressors for button presses modeled as stick/delta functions, picture presentations modeled with an epoch/boxcar function (duration: 2.5 s), and rating scales modeled with an epoch/boxcar function of variable duration (depending on when the subsequent button press occurred). The contrast between brain activity during viewing of IAPS pictures versus viewing scrambled pictures was calculated individually using a fixed effects model (first-level analysis, meaningful vs scrambled pictures).

Construction of a Population-Average Anatomical Probabilistic Atlas: Automatic segmentation of the subjects' T1-weighted images was used to build a population-average probabilistic anatomical atlas. More precisely, each participant's T1-weighted image was first automatically segmented into cortical and subcortical structures using FreeSurfer (version 4.5, http:// surfer.nmr.mgh.harvard.edu/).[4] Labeling of the cortical gyri was based on the Desikan-Killiany Atlas,[5], yielding 35 regions per hemisphere. The segmented T1 image was then normalized to the study-specific anatomical template space using the subject's previously computed warp field and affine-registered to the MNI space. The normalized segmentations were finally averaged across subjects, in order to create a population-average probabilistic atlas. Each voxel of the template could consequently be assigned a probability of belonging to a given anatomical structure, based on the individual information from 1000 subjects.

VBM analysis: Quantitative assessment of regional gray matter (GM) volume variations across subjects was performed using voxel based morphometry (VBM) and DARTEL[6], as implemented in the VBM8 toolbox of SPM8 (Statistical Parametric Mapping, Wellcome Trust Centre for Neuroimaging, London, UK; http://www.fil.ion.ucl.ac.uk/spm/). Of the 1119 subjects included in the fMRI analysis, the T1 images of 2 subjects were excluded due to subtle movement or noise artifacts that could affect the VBM procedure. Spatial normalization to the MNI space was done using the "modulated non-linear only" option, allowing the comparison of absolute amount of tissue corrected for individual brain sizes. Images were finally smoothed with a 8 mm FWHM isotropic Gaussian kernel. A regression model was used to analyze associations between gray matter volume and the multi-allelic score, including age and gender as covariates. Similarly as for the fMRI analysis, a SVC mask consisting of the left and right atlas-based hippocampi voxels in which the probability exceeded a threshold of 50% was applied. Statistical significance was assessed at $P(\text{FWE})<0.05$ within this region.

Detailed description of fMRI group statistics

More precisely, the small volume correction (SVC) mask consisted of the left and right hippocampi voxels in which the probability exceeded a threshold of 50%. Within these ROIs, SVC for multiple comparison was applied at a threshold of $P<0.05$. We used GLM Flex (Martinos Center & Mass General Hospital, Charlestown, MA, USA; http://mrtools.mgh.harvard.edu/) for the second-level analyses, as EPI sequences suffer from signal loss in the presence of magnetic field inhomogeneities that can occur close to air-tissue boundaries. The normalization procedure applied in DARTEL accurately transforms both voxels with signal and voxels with signal loss to MNI space. In SPM8, signal loss at a MNI

coordinate in a functional image of only one subject leads to the exclusion of the voxel at this coordinate from the group level analysis. Therefore, the probability of a voxel being excluded increases with sample size. GLM Flex circumvents this problem by allowing a variable number of subjects at each voxel. The minimum number of subjects per voxel was set to be 500.

Alternative pathway algorithm: INRICH

INRICH[7] is robust to potential confounders (i.e. varying gene and gene-set sizes and LD structure of GWAS SNPs). The INRICH algorithm counts the number of overlaps between independent intervals (clumping threshold in PLINK was set to $P < 0.005$, interval size ≤ 500kb and $r^2 = 0.2$) of LD, harboring the strongest association signals of a GWAS and predefined gene-sets. This overlap (i.e. a real number) is then corrected with permutation-based methods, by randomly drawing intervals, which match the observed intervals in size, and then calculating an empirical *P* value as percentage of random intervals showing at least same overlap as the observed overlap. The empirical *P* value is corrected for the number of gene-sets that have been tested in the same analysis via bootstrapping. First, we used the –clump option in PLINK to define independent intervals harboring the best GWAS association signals. We ran INRICH with 100000 permutations and 10000 bootstrapping samples. As in MAGENTA, the target gene borders were set to ±0kb, and the gene-set size ranged between 20 and 200 target genes. Finally, 177 KEGG gene-sets provided by the INRICH software (MsigDB v3.0) were tested.

In addition to the Calcium Signaling Pathway gene set, following KEGG gene sets were significantly enriched:

Discovery sample: Purine Metabolism, Pyrimidine Metabolism, Homologous Recombination, Gap Junction, Pancreatic Secretion, Endometrial Cancer, Primary Immunodeficiency. Replication sample: Glycosphingolipid Biosynthesis-globo series, Homologous Recombination, Non-homologous End-joining.

Ingenuity® Pathway Analysis

Data were also analyzed with QIAGEN's Ingenuity® Pathway Analysis software package (IPA®, QIAGEN Redwood City, www.qiagen.com/ingenuity). Specifically, IPA was used to estimate the enrichment of the EM core gene set with molecules listed in IPA's curated catalogue of Bio Functions and to compare such enrichment with the group of 66 non-contributing genes. Thus, we searched for Bio Functions showing highest enrichment in the EM core gene set and the largest difference in enrichment between the EM core gene set and the group of 66 non-contributing genes. The top Bio Function category fulfilling this criterion was "elevation of cytosolic calcium" (enrichment in the EM core gene set: 42.3% of the genes, $P=8.9 \times 10^{-18}$; enrichment in the group of 66 non-contributing genes: 10.6% of the genes, $P=2.7 \times 10^{-7}$). The second Bio Function category fulfilling this criterion was "G-protein signaling, coupled to IP3 second messenger (phospholipase C activating)" (enrichment in the EM core gene set: $P=2.5 \times 10^{-9}$; enrichment in the group of 66 non-contributing genes: $P=0.0003$). The third such category was "efflux of Ca^{2+}" (enrichment in the EM core gene set: $P=1.5 \times 10^{-8}$; enrichment in the group of 66 non-contributing genes: $P=0.00004$).

eFigure 1

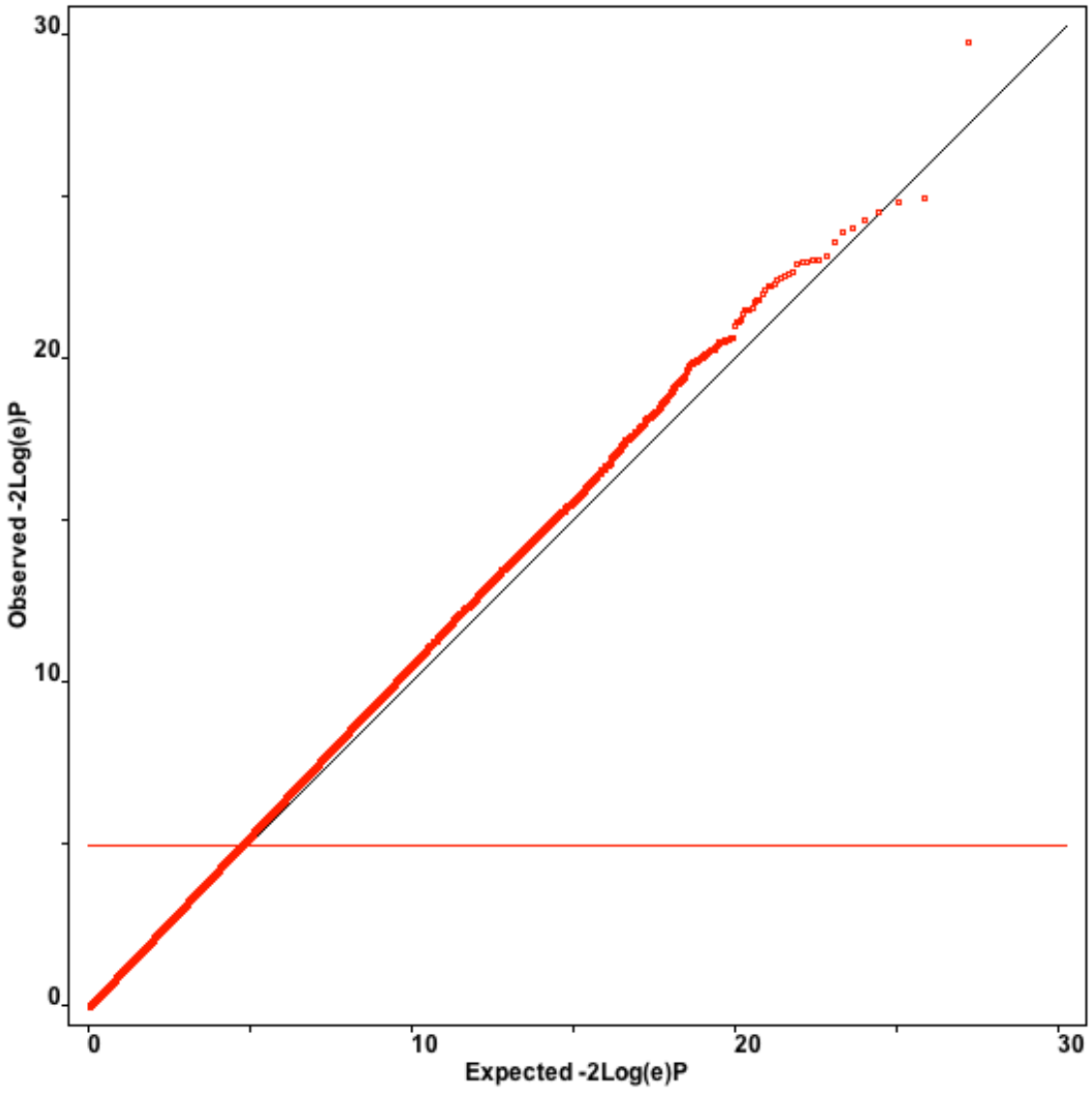

eFigure 2

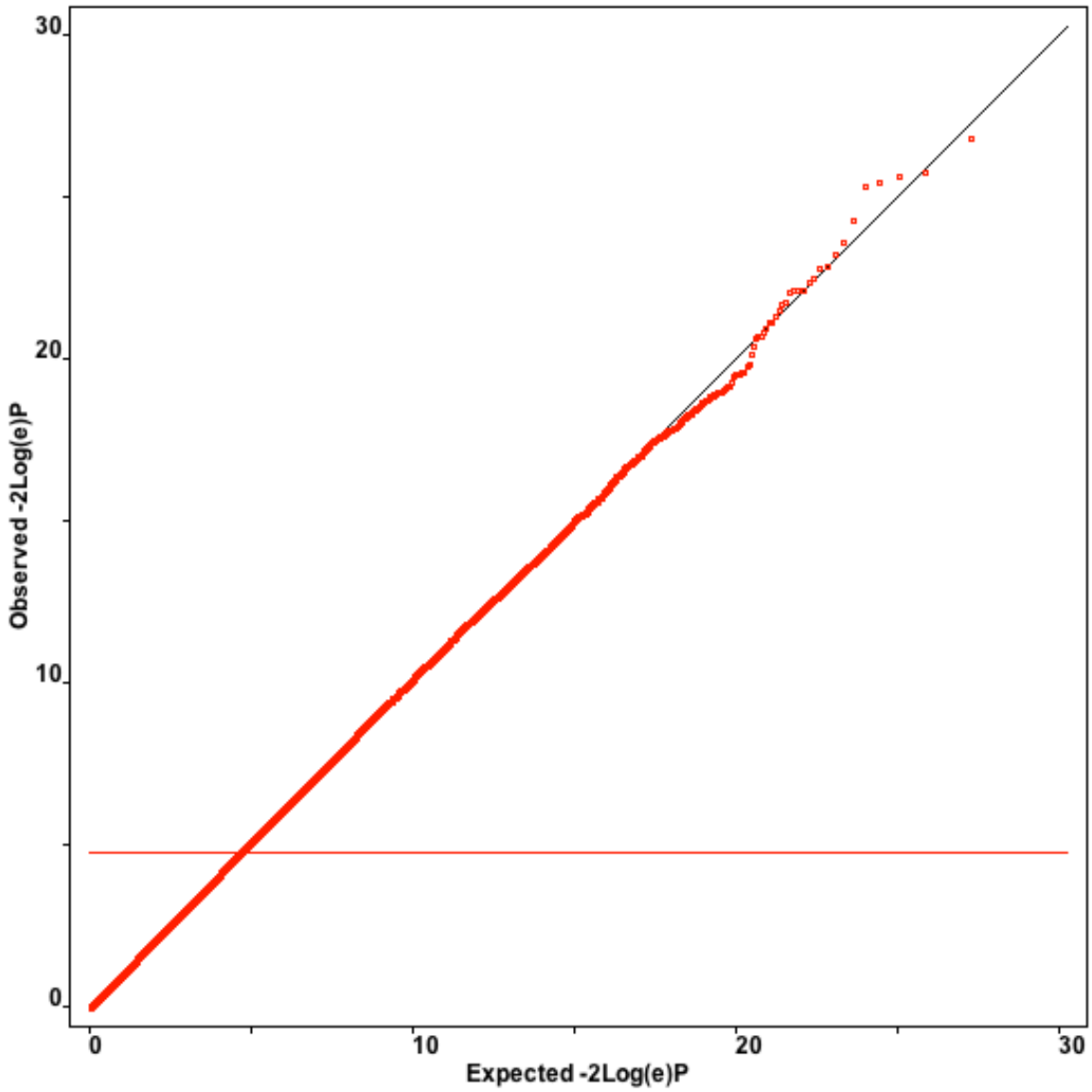

eFigure 3

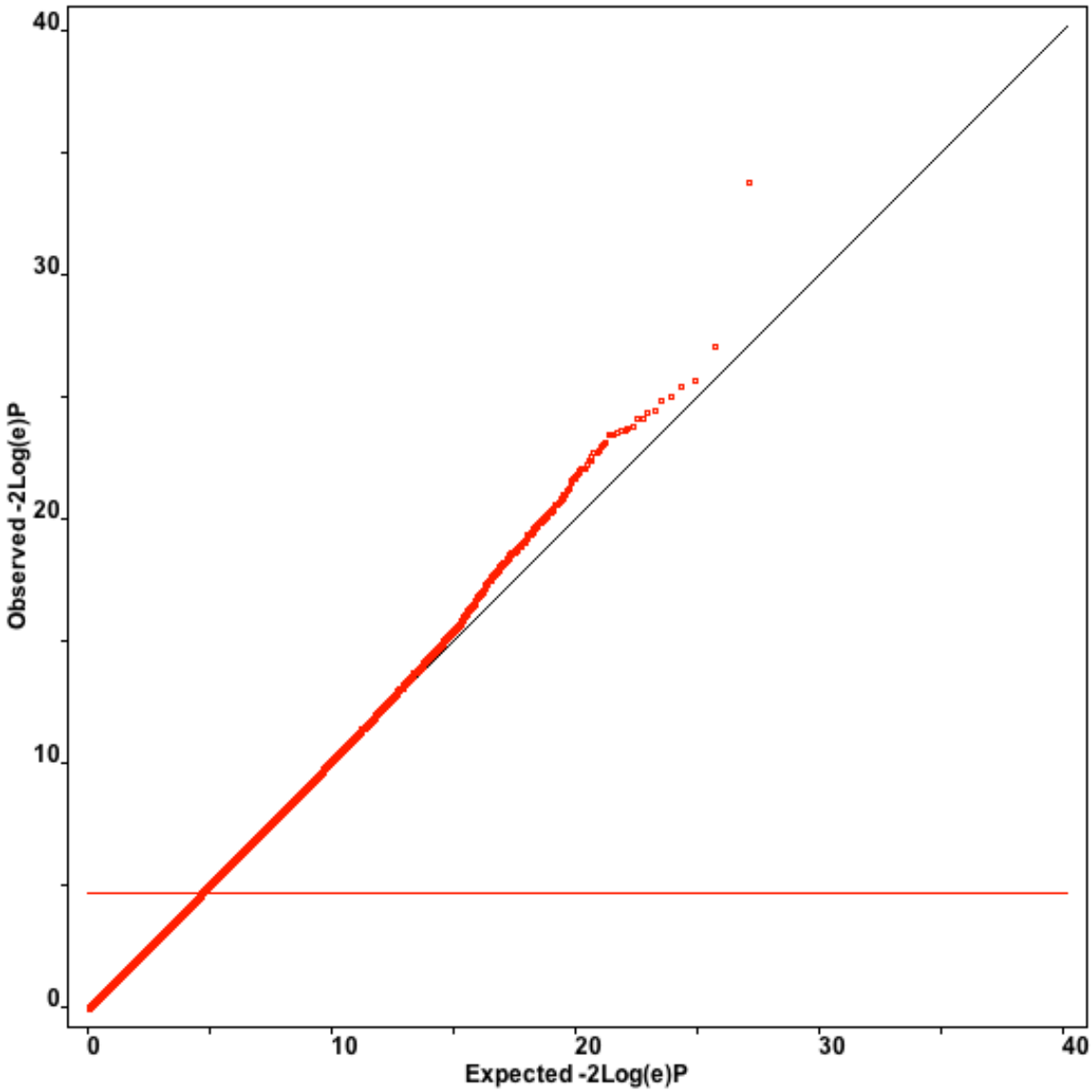

eFigure 4

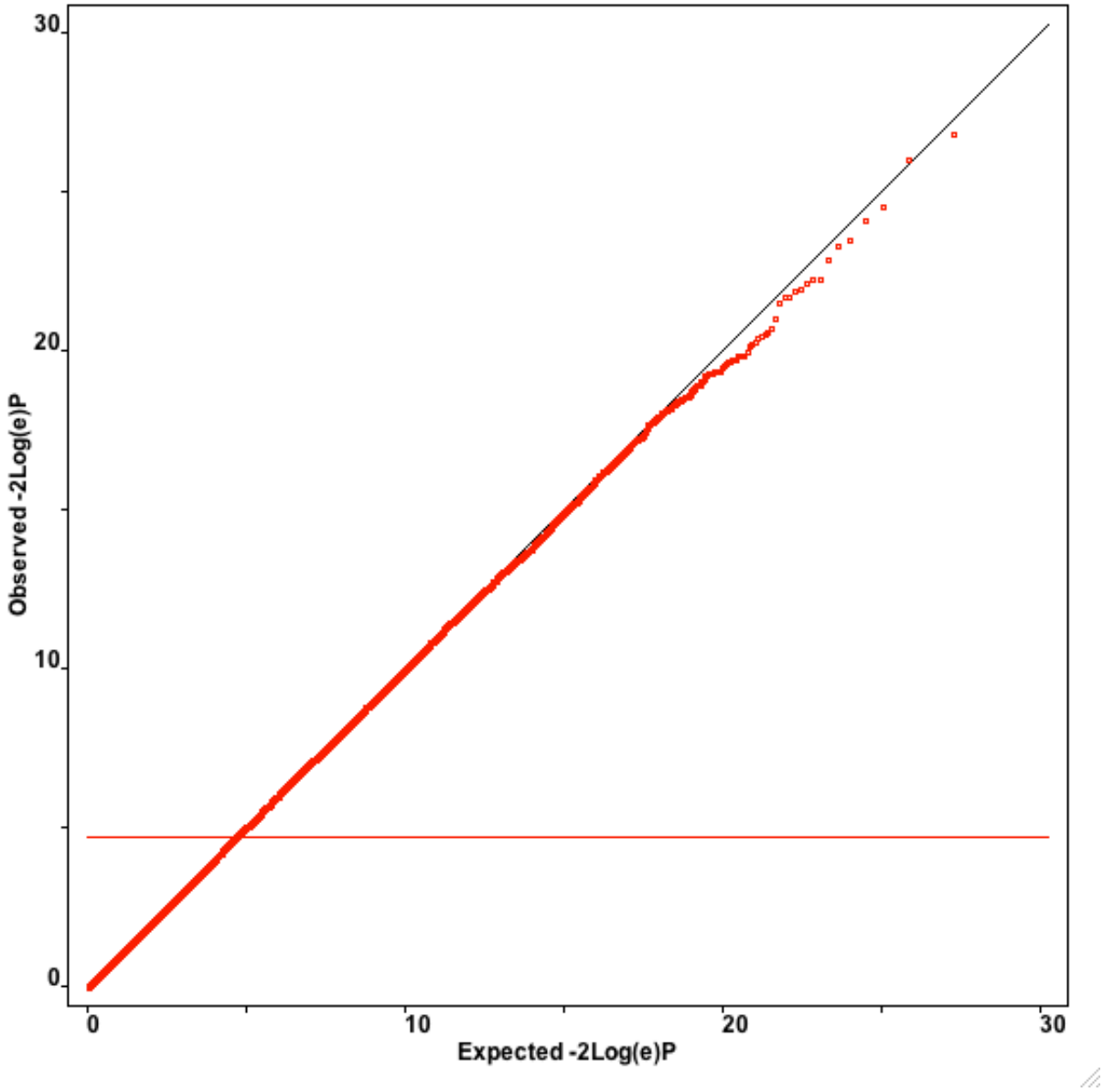

eFigure 5

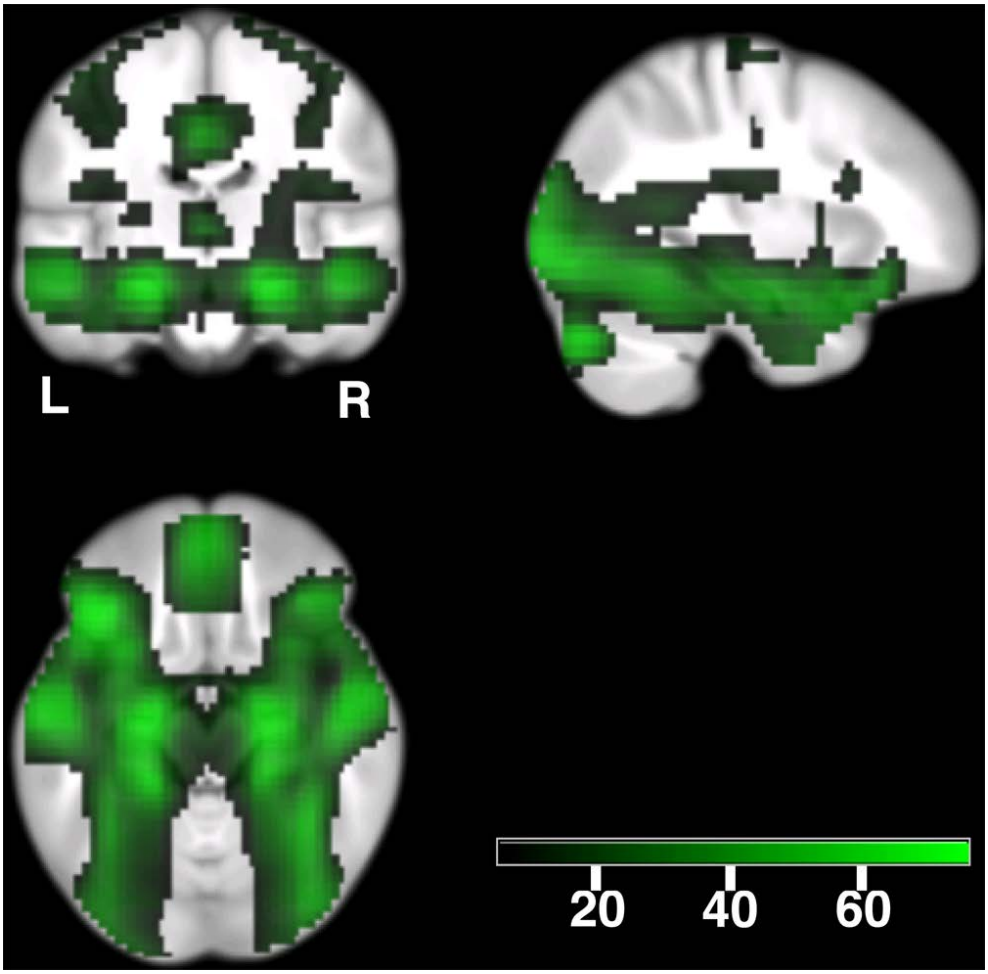

Legend: Color-coded t values ($P_{\text{whole-brain -FWE-corrected}} < 0.05$; n=1119). The map is centered at [33 -16.5 -16] in the right hippocampus. Activations are overlaid on coronal (upper left), sagittal (upper right) and axial (lower left) sections of the study specific group template (see Methods). L, left side of the brain; R, right side of the brain.

eTable 1. Demographics of the cognitively healthy samples

	Discovery sample	Replication sample	Zurich sample	AgeCoDe sample
Age (mean ± SD)	22.5 ± 3.5	22.5 ± 3.3	21.2 ± 1.9	79.5 ± 3.02
Gender (% female)	66.6	60	72.4	67.8

eTable 2. Multilocus genetic score: Gene symbols, SNP IDs, reference allele, major allele and direction of effect on EM performance in the discovery sample

Gene	SNP ID	Reference allele	Major allele	Direction of effect
ADCY9	rs437187	A	C	+
ADRA1A	rs7017961	A	G	+
BST1	rs4326008	T	G	+
CACNA1A	rs1120559	T	C	-
CACNA1B	rs10867100	A	C	-
CCKBR	rs2947025	C	G	+
CHRM1	rs2067478	A	G	+
CHRM5	rs2684932	T	C	-
HTR2A	rs927544	C	T	+
MYLK	rs1254389	A	T	-
NOS3	rs3918188	T	G	+
PDE1B	rs884510	C	T	-
PDGFRA	rs13147194	C	A	+
SLC8A3	rs227434	A	C	+
TRPC1	rs13081200	G	C	+

eTable 3. EM core gene set

Symbol	Entrez Gene Name	Chr	Start (bp)	End (bp)	Location	Type(s)	GeneCards® Description
ADCY8	adenylate cyclase 8 (brain)	16	4012649	4166186	plasma membrane	enzyme	Adenylyl Cyclases (AC) are a group of enzymes that convert adenosine-5'-triphosphate (ATP) into3',5'-adenosine monophosphate (cAMP) and pyrophosphate. There are ten different mammalian isoforms of AC; nine are membrane-bound, which are all found in, but not limited to, excitable tissues such as neurons and muscle, and one soluble form (sAC), which is expressed predominantly in the testis. The ten adenylyl cyclase isoforms can be divided into five distinct families based on their functional attributes; AC1, AC3 and AC8 are Ca2+-calmodulin-sensitive; AC2, AC4 and AC7 are Gbetagamma-stimulatory forms; AC5 and AC6 are distinguished by their insensitivity to inhibition by both Ca2+ and Galphai; AC9 is forskolin-insensitive and sAC is similar to cyanobacteria AC. Adenylyl cyclases are regulated by post-translational modifications, phosphorylation, G proteins, forskolin, pyrophosphate, calcium and calmodulin and the functions of this enzyme are diverse. Perturbations in adenylyl cyclase activity has been implicated in alcholol and opioid addiction and is associated with human diseases, including thyroid adenoma, male precocious puberty and chondrodysplasia.
ADRA1A	adrenoceptor alpha 1A	8	26605666	26722922	plasma membrane	G-protein coupled receptor	Adrenergic alpha1 receptors (alpha1-adrenoceptors) are members of the adrenergic receptor group of G-protein-coupled receptors that also includes alpha2A, alpha2B, alpha2C, beta1, beta2 and beta3. The adrenergic alpha1 receptors are further divided into three subtypes: alpha1A, alpha1B and alpha1D receptors. Alpha1-adrenoceptors are widely distributed in both the CNS and periphery where they play a major role in smooth muscle contraction. A fourth alpha1 receptor subtype has been postulated and is designated as alpha1L based on its low affinity for prazosin. It has been suggested that this subtype may represent a different conformational state of the alpha1A subtype.

ATP2B4	ATPase, Ca++ transporting, plasma membrane 4	1	203595927	203713209	plasma membrane	transporter	The protein encoded by this gene belongs to the family of P-type primary ion transport ATPases characterized by the formation of an aspartyl phosphate intermediate during the reaction cycle. These enzymes remove bivalent calcium ions from eukaryotic cells against very large concentration gradients and play a critical role in intracellular calcium homeostasis. The mammalian plasma membrane calcium ATPase isoforms are encoded by at least four separate genes and the diversity of these enzymes is further increased by alternative splicing of transcripts. The expression of different isoforms and splice variants is regulated in a developmental, tissue- and cell type-specific manner, suggesting that these pumps are functionally adapted to the physiological needs of particular cells and tissues. This gene encodes the plasma membrane calcium ATPase isoform 4. Alternatively spliced transcript variants encoding different isoforms have been identified.
AVPR1A	arginine vasopressin receptor 1A	12	63540215	63546590	plasma membrane	G-protein coupled receptor	The protein encoded by this gene acts as receptor for arginine vasopressin. This receptor belongs to the subfamily of G-protein coupled receptors which includes AVPR1B, V2R and OXT receptors. Its activity is mediated by G proteins which stimulate a phosphatidylinositol-calcium second messenger system. The receptor mediates cell contraction and proliferation, platelet aggregation, release of coagulation factor and glycogenolysis. Diseases associated with AVPR1A include autism, and adenomyosis.
CACNA1E	calcium channel, voltage-dependent, R type, alpha 1E subunit	1	181452715	181770715	plasma membrane	ion channel	Voltage-dependent calcium channels are multisubunit complexes consisting of alpha-1, alpha-2, beta, and delta subunits in a 1:1:1:1 ratio. These channels mediate the entry of calcium ions into excitable cells, and are also involved in a variety of calcium-dependent processes, including muscle contraction, hormone or neurotransmitter release, gene expression, cell motility, cell division and cell death. This gene encodes the alpha-1E subunit of the R-type calcium channels, which belong to the 'high-voltage activated' group that maybe involved in the modulation of firing patterns of neurons important for information processing. Alternatively spliced transcript variants encoding

							different isoforms have been described for this gene. Diseases associated with CACNA1E include migraine. GO annotations related to this gene include voltage-gated calcium channel activity and calcium ion binding.
CACNA1G	calcium channel, voltage-dependent, T type, alpha 1G subunit	17	48638448	48704542	plasma membrane	ion channel	This gene encodes a T-type, low-voltage activated calcium channel. The T-type channels generate currents that are both transient, owing to fast inactivation, and tiny, owing to small conductance. T-type channels are thought to be involved in pacemaker activity, low-threshold calcium spikes, neuronal oscillations and resonance, and rebound burst firing. Many alternatively spliced transcript variants encoding different isoforms have been described for this gene.
CACNA1S	calcium channel, voltage-dependent, L type, alpha 1S subunit	1	201008639	201081694	plasma membrane	ion channel	This gene encodes one of the five subunits of the slowly inactivating L-type voltage-dependent calcium channel in skeletal muscle cells. Mutations in this gene have been associated with hypokalemic periodic paralysis, thyrotoxic periodic paralysis and malignant hyperthermia susceptibility.
CAMK2G	calcium/calmodulin-dependent protein kinase II gamma	10	75572258	75634343	cytoplasm	kinase	The product of this gene is one of the four subunits of an enzyme which belongs to the serine/threonine protein kinase family, and to the Ca(2+)/calmodulin-dependent protein kinase subfamily. Calcium signaling is crucial for several aspects of plasticity at glutamatergic synapses. In mammalian cells the enzyme is composed of four different chains: alpha, beta, gamma, and delta. The product of this gene is a gamma chain. Many alternatively spliced transcripts encoding different isoforms have been described but the full-length nature of all the variants has not been determined.
CCKBR	cholecystokinin B receptor	11	6280965	6293356	plasma membrane	G-protein coupled receptor	This gene encodes a G-protein coupled receptor for gastrin and cholecystokinin (CCK), regulatory peptides of the brain and gastrointestinal tract. This protein is a type B gastrin receptor, which has a high affinity for both sulfated and nonsulfated CCK analogs and is found principally in the central nervous system and the gastrointestinal tract. A misspliced transcript variant including an intron has been observed in cells from colorectal and pancreatic tumors. Diseases associated with CCKBR include agoraphobia, and duodenal

							gastrinoma.
CHRM5	cholinergic receptor, muscarinic 5	15	34261088	34357287	plasma membrane	G-protein coupled receptor	The muscarinic cholinergic receptors belong to a larger family of G protein-coupled receptors. The functional diversity of these receptors is defined by the binding of acetylcholine and includes cellular responses such as adenylate cyclase inhibition, phosphoinositide degeneration, and potassium channel mediation. Muscarinic receptors influence many effects of acetylcholine in the central and peripheral nervous system. Stimulation of this receptor is known to increase cyclic AMP levels. Diseases associated with CHRM5 include cannabis dependence, and schizophrenia.
GNA15	guanine nucleotide binding protein (G protein), alpha 15 (Gq class)	19	3136190	3163766	plasma membrane	enzyme	GNA15 is a protein-coding gene. GO annotations related to this gene include GTP binding and GTPase activity. An important paralog of this gene is GNAQ.
HTR2A	5-hydroxytryptamine (serotonin) receptor 2A, G protein-coupled	13	47407512	47471169	plasma membrane	G-protein coupled receptor	This gene encodes one of the receptors for serotonin, a neurotransmitter with many roles. Mutations in this gene are associated with susceptibility to schizophrenia and obsessive-compulsive disorder, and are also associated with response to the antidepressant citalopram in patients with major depressive disorder (MDD). MDD patients who also have a mutation in intron 2 of this gene show a significantly reduced response to citalopram as this antidepressant downregulates expression of this gene. Multiple transcript variants encoding different isoforms have been found for this gene.
ITPKB	inositol-trisphosphate 3-kinase B	1	226819390	226926876	cytoplasm	kinase	The protein encoded by this protein regulates inositol phosphate metabolism by phosphorylation of second messenger inositol 1,4,5-trisphosphate to Ins(1,3,4,5)P4. The activity of this encoded protein is responsible for regulating the levels of a large number of inositol polyphosphates that are important in cellular signaling. Both calcium/calmodulin and protein phosphorylation mechanisms control its activity.
ITPR1	inositol 1,4,5-trisphosphate	3	4535031	4889524	cytoplasm	ion channel	This gene encodes an intracellular receptor for inositol 1,4,5-trisphosphate. Upon stimulation by inositol 1,4,5-trisphosphate,

	receptor, type 1						this receptor mediates calcium release from the endoplasmic reticulum. Mutations in this gene cause spinocerebellar ataxia type 15, a disease associated with an heterogeneous group of cerebellar disorders. Multiple transcript variants have been identified for this gene.
P2RX7	purinergic receptor P2X, ligand-gated ion channel, 7	12	121570621	121624354	plasma membrane	ion channel	The product of this gene belongs to the family of purinoceptors for ATP. This receptor functions as a ligand-gated ion channel and is responsible for ATP-dependent lysis of macrophages through the formation of membrane pores permeable to large molecules. Activation of this nuclear receptor by ATP in the cytoplasm may be a mechanism by which cellular activity can be coupled to changes in gene expression. Multiple alternatively spliced variants have been identified, most of which fit nonsense-mediated decay (NMD) criteria.
PDGFRA	platelet-derived growth factor receptor, alpha polypeptide	4	55095263	55164412	plasma membrane	kinase	This gene encodes a cell surface tyrosine kinase receptor for members of the platelet-derived growth factor family. These growth factors are mitogens for cells of mesenchymal origin. The identity of the growth factor bound to a receptor monomer determines whether the functional receptor is a homodimer or a heterodimer, composed of both platelet-derived growth factor receptor alpha and beta polypeptides. Studies suggest that this gene plays a role in organ development, wound healing, and tumor progression. Mutations in this gene have been associated with idiopathic hypereosinophilic syndrome, somatic and familial gastrointestinal stromal tumors, and a variety of other cancers.
PDGFRB	platelet-derived growth factor receptor, beta polypeptide	5	149493401	149535422	plasma membrane	kinase	This gene encodes a cell surface tyrosine kinase receptor for members of the platelet-derived growth factor family. It is flanked on chromosome 5 by the genes for granulocyte-macrophage colony-stimulating factor and macrophage-colony stimulating factor receptor; all three genes may be implicated in the 5-q syndrome. A translocation between chromosomes 5 and 12, that fuses this gene to that of the translocation, ETV6, leukemia gene, results in chronic myeloproliferative disorder with eosinophilia.
PLCB2	phospholipase C, beta 2	4	101944586	102268628	cytoplasm	enzyme	The production of the second messenger molecules diacylglycerol (DAG) and inositol 1,4,5-trisphosphate (IP3) is mediated by activated phosphatidylinositol-specific

							phospholipase C enzymes. PLCB2 is a protein-coding gene. Diseases associated with PLCB2 include platelet plc beta-2 deficiency, and prostate leiomyosarcoma.
PLCD4	phospholipase C, delta 4	2	219472487	219501909	cytoplasm	enzyme	This gene encodes a member of the delta class of phospholipase C enzymes. Phospholipase C enzymes play a critical role in many cellular processes by hydrolyzing phosphatidylinositol 4,5-bisphosphate into two intracellular second messengers, inositol 1,4,5-trisphosphate and diacylglycerol. Expression of this gene may be a marker for cancer.
PLCG2	phospholipase C, gamma 2 (phosphatidylinositol-specific)	16	81812929	81991899	cytoplasm	enzyme	The protein encoded by this gene is a transmembrane signaling enzyme that catalyzes the conversion of 1-phosphatidyl-1D-myo-inositol 4,5-bisphosphate to 1D-myo-inositol 1,4,5-trisphosphate (IP3) and diacylglycerol (DAG) using calcium as a cofactor. IP3 and DAG are second messenger molecules important for transmitting signals from growth factor receptors and immune system receptors across the cell membrane. Mutations in this gene have been found in autoinflammation, antibody deficiency, and immune dysregulation syndrome and familial cold autoinflammatory syndrome 3.
PPP3CA	protein phosphatase 3, catalytic subunit, alpha isozyme	4	101944586	102268628	cytoplasm	phosphatase	Calcium-dependent, calmodulin-stimulated protein phosphatase. This subunit may have a role in the calmodulin activation of calcineurin.
PPP3R1	protein phosphatase 3, regulatory subunit B, alpha	2	68405988	68479651	cytoplasm	phosphatase	Regulatory subunit of calcineurin, a calcium-dependent, calmodulin stimulated protein phosphatase. Confers calcium sensitivity. Diseases associated with PPP3R1 include calcaneonavicular coalition.
PRKCB	protein kinase C, beta	16	23847299	24231932	cytoplasm	kinase	Protein kinase C (PKC) is a family of serine- and threonine-specific protein kinases that can be activated by calcium and second messenger diacylglycerol. PKC family members phosphorylate a wide variety of protein targets and are known to be involved in diverse cellular signaling pathways. PKC family members also serve as major receptors for phorbol esters, a class of tumor promoters. Each member of the PKC family has a specific expression profile and is believed to play a distinct role in cells. The protein encoded by this gene is one of the PKC family members. This protein kinase has been reported to be involved in

							many different cellular functions, such as B cell activation, apoptosis induction, endothelial cell proliferation, and intestinal sugar absorption. Studies in mice also suggest that this kinase may also regulate neuronal functions and correlate fear-induced conflict behavior after stress. Alternatively spliced transcript variants encoding distinct isoforms have been reported.
PTGER3	prostaglandin E receptor 3 (subtype EP3)	1	71318035	71513491	plasma membrane	G-protein coupled receptor	The protein encoded by this gene is a member of the G-protein coupled receptor family. This protein is one of four receptors identified for prostaglandin E2 (PGE2). This receptor may have many biological functions, which involve digestion, nervous system, kidney reabsorption, and uterine contraction activities. Studies of the mouse counterpart suggest that this receptor may also mediate adrenocorticotropic hormone response as well as fever generation in response to exogenous and endogenous stimuli. Multiple transcript variants encoding different isoforms have been found for this gene.
RYR3	ryanodine receptor 3	15	33603176	34158303	plasma membrane	ion channel	The protein encoded by this gene is a ryanodine receptor, which functions to release calcium from intracellular storage for use in many cellular processes. For example, the encoded protein is involved in skeletal muscle contraction by releasing calcium from the sarcoplasmic reticulum followed by depolarization of T-tubules. Two transcript variants encoding different isoforms have been found for this gene. Diseases associated with RYR3 include central core myopathy, and neuroleptic malignant syndrome.
TACR1	tachykinin receptor 1	2	75273589	75426645	plasma membrane	G-protein coupled receptor	This gene belongs to a gene family of tachykinin receptors. These tachykinin receptors are characterized by interactions with G proteins and contain seven hydrophobic transmembrane regions. This gene encodes the receptor for the tachykinin substance P, also referred to as neurokinin 1. The encoded protein is also involved in the mediation of phosphatidylinositol metabolism of substance P.

Abbreviations: chr, chromosome

eTable 4. Detailed information about the GSEA results in the discovery and the replication sample: gene *P* value, chromosome, gene start, gene end, most significant SNP, SNP *P* value, effect size, frequency

Gene	Gene p-value	Chr	Start (bp)	End (bp)	Most significant SNP	*P* value	Effect size	Frequency
Discovery sample								
ADCY2	2.21E-01	5	7396342	7830194	rs2914296	2.76E-03	-1.19	0.17
ADCY4	1.78E-01	14	24787554	24804277	rs10483285	3.93E-02	1.29	0.06
ADCY8	1.91E-01	8	131792546	132052835	rs16904358	8.14E-03	-1.01	0.18
ADCY9	1.79E-02	16	4012649	4166186	rs437187	1.30E-03	1.66	0.09
ADRA1A	3.95E-02	8	26605666	26722922	rs7017961	3.69E-03	0.94	0.33
ADRA1B	9.70E-02	5	159343739	159400017	rs7718362	1.64E-02	-2.30	0.02
ADRA1D	2.01E-01	20	4201277	4229659	rs4815675	4.70E-02	0.60	0.41
ATP2A2	1.57E-01	12	110719031	110788897	rs17187412	3.09E-02	-1.13	0.09
ATP2B2	1.91E-01	3	10365706	10547268	rs4684697	1.37E-02	0.76	0.35
ATP2B4	1.23E-01	1	203595927	203713209	rs2236550	1.40E-02	-3.06	0.01
AVPR1A	1.44E-01	12	63540215	63546590	rs11174811	3.89E-02	0.93	0.12
BST1	6.51E-03	4	15704572	15733796	rs4326008	1.53E-03	1.13	0.23
CACNA1A	3.55E-02	19	13317255	13617274	rs1120559	7.50E-04	-1.56	0.12
CACNA1B	2.05E-02	9	140772240	141019076	rs10867100	7.77E-04	-3.76	0.02
CACNA1E	1.97E-01	1	181452715	181770715	rs16857594	5.86E-03	-1.50	0.08
CACNA1G	2.08E-01	17	48638448	48704542	rs9898731	3.95E-02	-0.61	0.45
CACNA1S	2.08E-01	1	201008639	201081694	rs9427468	2.72E-02	0.80	0.22
CAMK2G	9.04E-02	10	75572258	75634343	rs7080350	1.70E-02	0.72	0.42
CAMK4	2.91E-01	5	110559946	110820748	rs9285875	1.72E-02	-0.81	0.27
CCKBR	7.61E-03	11	6280965	6293356	rs2947025	1.44E-03	1.12	0.23
CHRM1	4.09E-03	11	62676150	62689012	rs2067478	1.25E-03	2.64	0.03
CHRM3	5.93E-02	1	239792372	240072717	rs10925994	1.54E-03	-1.52	0.11
CHRM5	4.41E-02	15	34261088	34357287	rs2684932	5.45E-03	-1.09	0.17
EGFR	1.48E-01	7	55086724	55275031	rs11487218	9.89E-03	0.79	0.35
GNA15	1.27E-01	19	3136190	3163766	rs2074865	2.49E-02	-0.96	0.13
GNAQ	1.47E-01	9	80335190	80646219	rs17063991	4.71E-03	2.05	0.05
GRIN2A	2.31E-01	16	9847264	10276611	rs4782108	2.85E-03	-1.13	0.20
GRM1	9.52E-02	6	146348781	146758731	rs7748653	1.08E-03	-2.70	0.03
HTR2A	1.96E-02	13	47407512	47471169	rs927544	2.27E-03	1.02	0.26
ITPKB	2.12E-01	1	226819390	226926876	rs1144838	2.99E-02	1.04	0.11
ITPR1	9.85E-02	3	4535031	4889524	rs4684427	1.29E-03	0.94	0.50
ITPR2	1.74E-01	12	26488284	26986131	rs16930558	1.03E-03	-4.47	0.01
ITPR3	2.54E-01	6	33589155	33664348	rs3818528	4.26E-02	-0.65	0.31
LHCGR	2.33E-01	2	48913912	48982880	rs12618729	3.50E-02	0.87	0.15
MYLK	3.08E-02	3	123331142	123603149	rs1254389	9.45E-04	-2.18	0.05
MYLK2	1.41E-01	20	30407177	30422500	rs6058470	3.60E-02	0.76	0.21
NOS3	1.64E-03	7	150688143	150711687	rs3918188	5.76E-04	1.07	0.33
NTSR1	1.14E-01	20	61340188	61394123	rs8126434	1.85E-02	-2.38	0.02
OXTR	2.40E-01	3	8792094	8811300	rs2268495	4.40E-02	0.73	0.22
P2RX5	2.49E-01	17	3576521	3599583	rs149245	5.67E-02	-0.59	0.40
P2RX7	1.73E-01	12	121570621	121624354	rs6489794	2.73E-02	0.96	0.14
PDE1B	2.63E-03	12	54943176	54973023	rs884510	7.26E-04	-1.02	0.34
PDGFRA	8.61E-03	4	55095263	55164412	rs13147194	1.65E-03	1.30	0.15
PDGFRB	2.23E-01	5	149493401	149535422	rs4324662	4.28E-02	-0.71	0.23
PLCB2	1.82E-01	15	40580097	40600174	rs3784397	4.30E-02	-0.61	0.41
PLCD4	7.14E-02	2	219472487	219501909	rs12989189	1.69E-02	-1.09	0.12

PLCG2	1.37E-01	16	81812929	81991899	rs8053418	8.20E-03	-1.43	0.08
PPP3CA	1.70E-01	4	101944586	102268628	rs2850986	4.83E-03	0.98	0.24
PPP3R1	5.51E-02	2	68405988	68479651	rs6546359	9.46E-03	0.89	0.24
PRKCB	2.01E-01	16	23847299	24231932	rs2188354	3.48E-03	-2.20	0.04
PTAFR	5.25E-02	1	28473676	28520447	rs905907	1.12E-02	1.92	0.04
PTGER3	1.22E-01	1	71318035	71513491	rs10443262	7.88E-03	-0.80	0.40
PTGFR	2.74E-01	1	78956727	79006386	rs3766331	5.81E-02	2.24	0.02
RYR3	2.05E-01	15	33603176	34158303	rs11854602	6.79E-04	-2.77	0.03
SLC8A1	2.45E-01	2	40339285	40739575	rs11895025	4.02E-03	-1.22	0.13
SLC8A3	5.50E-04	14	70510933	70655787	rs227434	5.32E-05	1.18	0.47
TACR1	8.53E-02	2	75273589	75426645	rs1106855	6.89E-03	0.89	0.27
TRPC1	2.57E-02	3	142443265	142526729	rs13081200	4.28E-03	1.05	0.21
Replication sample								
ADCY3	8.31E-02	2	25042038	25142055	rs10195271	1.22E-02	0.97	0.29
ADCY8	1.59E-01	8	131792546	132052835	rs11990501	7.32E-03	3.94	0.01
ADRA1A	2.01E-01	8	26605666	26722922	rs12542523	2.60E-02	-1.70	0.05
ATP2B4	5.53E-02	1	203595927	203713209	rs11580986	6.64E-03	-0.93	0.48
AVPR1A	1.28E-01	12	63540215	63546590	rs11174810	3.55E-02	-2.64	0.02
CACNA1E	8.48E-02	1	181452715	181770715	rs3843280	2.24E-03	-1.15	0.28
CACNA1G	5.63E-02	17	48638448	48704542	rs107067	1.07E-02	1.93	0.05
CACNA1I	8.57E-02	22	39966757	40085740	rs136848	1.13E-02	0.87	0.46
CACNA1S	1.28E-01	1	201008639	201081694	rs12403523	1.65E-02	1.57	0.07
CAMK2A	1.01E-01	5	149599053	149669403	rs10066581	1.74E-02	-1.23	0.13
CAMK2B	1.77E-01	7	44256748	44365230	rs10230538	2.93E-02	0.86	0.26
CAMK2G	1.21E-01	10	75572258	75634343	rs7080350	2.61E-02	-0.77	0.42
CCKAR	1.49E-01	4	26483017	26492042	rs915889	3.07E-02	-1.38	0.08
CCKBR	4.06E-02	11	6280965	6293356	rs2947025	7.48E-03	1.09	0.21
CHP2	7.70E-02	16	23765947	23770256	rs109592	2.36E-02	-0.96	0.21
CHRM5	2.49E-02	15	34261088	34357287	rs683470	3.65E-03	-2.95	0.03
CHRNA7	1.79E-01	15	32322690	32462384	rs8028396	2.21E-02	-0.84	0.37
EDNRA	1.92E-01	4	148402068	148466106	rs6537485	3.73E-02	-1.20	0.10
EDNRB	1.18E-01	13	78469615	78549664	rs4885493	2.08E-02	-0.87	0.28
GNA14	5.65E-02	9	80037994	80263232	rs1443868	2.80E-03	1.05	0.42
GNA15	1.98E-01	19	3136190	3163766	rs2074865	4.52E-02	-1.08	0.12
GNAL	1.24E-01	18	11689135	11883144	rs9951752	9.15E-03	-1.03	0.24
HRH2	1.28E-01	5	175085039	175113245	rs678591	3.23E-02	-1.94	0.04
HTR2A	1.50E-01	13	47407512	47471169	rs9534508	2.10E-02	-1.97	0.04
HTR5A	1.47E-01	7	154862545	154877459	rs2698513	2.62E-02	-1.91	0.04
ITPKB	1.04E-02	1	226819390	226926876	rs708774	1.54E-03	-1.21	0.29
ITPR1	2.06E-01	3	4535031	4889524	rs13092274	4.52E-03	-1.14	0.25
NOS1	3.54E-02	12	117645946	117799607	rs2682825	3.05E-03	-1.04	0.39
NOS2	1.43E-01	17	26083791	26127555	rs2297515	2.96E-02	1.03	0.16
P2RX4	2.38E-01	12	121647663	121671909	rs11610621	6.01E-02	-0.92	0.15
P2RX7	1.83E-04	12	121570621	121624354	rs2857585	7.29E-05	2.86	0.06
PDGFRA	5.55E-02	4	55095263	55164412	rs7677751	1.08E-02	-1.25	0.14
PDGFRB	1.03E-02	5	149493401	149535422	rs2007637	2.24E-03	1.47	0.16
PLCB2	1.21E-01	15	40580097	40600174	rs2305648	3.01E-02	-0.76	0.41
PLCD4	2.46E-01	2	219472487	219501909	rs7578554	6.94E-02	-3.14	0.01
PLCE1	1.97E-01	10	95753745	96088148	rs2689700	6.62E-03	1.24	0.18
PLCG2	1.93E-01	16	81812929	81991899	rs7499275	1.45E-02	-0.87	0.34
PLCZ1	8.11E-02	12	18836115	18890918	rs12300257	1.62E-02	-0.98	0.23
PLN	2.51E-02	6	118869441	118881587	rs12153955	7.17E-03	1.73	0.08
PPP3CA	1.01E-01	4	101944586	102268628	rs2659501	2.89E-03	-1.32	0.18
PPP3R1	1.85E-01	2	68405988	68479651	rs7599591	3.87E-02	0.77	0.36

PRKCB	1.20E-01	16	23847299	24231932	rs8056879	1.97E-03	-1.12	0.34
PTGER3	5.03E-02	1	71318035	71513491	rs7541936	3.33E-03	-1.47	0.13
PTK2B	6.62E-02	8	27168998	27316903	rs2322608	6.59E-03	1.21	0.17
RYR3	1.39E-01	15	33603176	34158303	rs680851	4.53E-04	-1.37	0.26
TACR1	8.63E-02	2	75273589	75426645	rs3771830	8.09E-03	-0.96	0.36
TNNC2	1.81E-01	20	44451854	44455953	rs4629	5.19E-02	-0.69	0.46
VDAC2	1.73E-01	10	76969911	76991207	rs12269517	4.31E-02	1.39	0.07

Abbreviation: chr, chromosome

eReferences.

1. Lang PJ, Bradley MM, Cuthbert BN. *International Affective Pictures System (IAPS): Affective Ratings of Pictures and Instruction Manual*. Gainesville, Fl.: University of Florida; 2008.

2. Welsh KA, Butters N, Mohs RC, et al. The Consortium to Establish a Registry for Alzheimer's Disease (CERAD). Part V. A normative study of the neuropsychological battery. *Neurology.* Apr 1994;44(4):609-614.

3. Lambert JC, Ibrahim-Verbaas CA, Harold D, et al. Meta-analysis of 74,046 individuals identifies 11 new susceptibility loci for Alzheimer's disease. *Nat Genet.* Dec 2013;45(12):1452-1458.

4. Fischl B, Salat DH, Busa E, et al. Whole brain segmentation: automated labeling of neuroanatomical structures in the human brain. *Neuron.* Jan 31 2002;33(3):341-355.

5. Desikan RS, Segonne F, Fischl B, et al. An automated labeling system for subdividing the human cerebral cortex on MRI scans into gyral based regions of interest. *Neuroimage.* Jul 1 2006;31(3):968-980.

6. Ashburner J. A fast diffeomorphic image registration algorithm. *Neuroimage.* Oct 15 2007;38(1):95-113.

7. Lee PH, O'Dushlaine C, Thomas B, Purcell SM. INRICH: interval-based enrichment analysis for genome-wide association studies. *Bioinformatics.* Jul 1 2012;28(13):1797-1799.